Nonlinear Dyn (2021) 106:867–877
https://doi.org/10.1007/s11071-021-06864-8

ORIGINAL PAPER

Abundant multilayer network model solutions and bright-dark solitons for a (3 + 1)-dimensional p-gBLMP equation

Litao Gai · Wen-Xiu Ma · Bilige Sudao

Received: 14 July 2021 / Accepted: 23 August 2021 / Published online: 9 September 2021

Abstract This paper aims to present a multilayer neural network model for a (3 + 1)-dimensional p-gBLMP equation. The generalized bilinear p-gBLMP equation is constructed, on the basis of the generalized bilinear operators. Through selecting different values in each layer, novel types of tensor functions can be furnished. We set the hidden neurons to some specific functions in some cases, and compute four types of new exact network model solutions for the p-gBLMP equation. The novelty and advantage of the proposed model are illustrated by applying to this model. Some plots of those presented new solutions are made to exhibit wave characteristics.

Keywords Multilayer neural network model · (3 + 1)-dimensional p-gBLMP equation · Generalized bilinear form

L. Gai · W.-X. Ma (✉)
Department of Mathematics, Zhejiang Normal University, Jinhua 321004, Zhejiang, China
e-mail: mawx@cas.usf.edu

L. Gai
e-mail: litaogai@zjnu.edu.cn

W.-X. Ma
Department of Mathematics, King Abdulaziz University, Jeddah 21589, Saudi Arabia

W.-X. Ma
Department of Mathematics and Statistics, University of South Florida, Tampa, FL 33620-5700, USA

W.-X. Ma
School of Mathematics, South China University of Technology, Guangzhou 510640, Guangdong, China

W.-X. Ma
School of Mathematical and Statistical Sciences, North-West University, Mafikeng Campus, Private Bag X2046, Mmabatho 2735, South Africa

B. Sudao
Department of mathematics, Inner Mongolia University of Technology, Hohhot 010051, Neimenggu, China
e-mail: inmathematica@126.com

1 Introduction

It is known that there are plenty of studies on a (2+1)-dimensional Boiti–Leon–Manna–Pempinelli (BLMP) equation

$$u_{yt} + u_{xxxy} - 3u_{xx}u_y - 3u_x u_{xy} = 0, \tag{1}$$

Equation (1) is usually used to describe incompressible fluid. A new fractional definition is used through the modified Khater method to get novel solitary wave solutions of this equation [1]. Some entirely new complexiton solutions and periodic-soliton solutions are derived by using an ansätz functions and the bilinear form [2]. Abundant interaction solutions between a lump and other multi-solitons are studied based on the Hirota bilinear method [3]. The analytical solutions are constructed through using the transformed rational function method and the $\exp(-\Phi(\xi))$ method [4]. Abundant exact and explicit solutions to Eq. (1) are constructed [5]. The transformed rational function method to construct different types of analytical solutions to Eq. (1) is studied [6]. Exact explicit solutions

of Eq. (1) are obtained by using these auto-Bäcklund transformation [7].

In recent years, scientists and researchers in general utilized the Hirota bilinear method for the purpose of solving nonlinear partial differential equations (NLPDEs) and obtaining the lump solutions [8–11], multiple soliton solutions [8,12,13], multi-lump solutions [14,15], interaction solutions [16,17], and others [18–20]. At the same time, the generalized forms of bilinear differential operators have also been widely used, which can transform bilinear equations into a variety of new forms [21]. The idea is to make a transformation into new variables, so that in those new variables, multi-soliton solutions or multi-parameter solutions are expressed in a particularly simple form.

In our work, we introduce a (3+1)-dimensional generalized Boiti–Leon–Manna–Pempinelli (gBLMP) equation

$$u_{xx} + u_{zt} + u_{yt} + u_{xxxy} - 3u_{xx}u_y - 3u_x u_{xy} = 0, \tag{2}$$

which can depict the evolution of Riemann wave propagation along the x-axis, y-axis and z-axis in incompressible fluid, respectively, where $u(x, y, z, t)$ denote the physical quantities in three directions of wave propagation, the extra terms u_{xx} and u_{zt} are added to Eq. (1). Consider the following first-order logarithmic transformation:

$$u = -\phi_x = -2[\ln f(x, y, z, t)]_x, \ \phi = 2\ln f(x, y, z, t), \tag{3}$$

substituting $u = -\phi_x$ into Eq. (2), one can be written as

$$\begin{aligned} &-\phi_{xxx} - \phi_{ztx} - \phi_{ytx} - \phi_{xxxxy} \\ &\quad -3\phi_{xxx}\phi_{xy} - 3\phi_{xx}\phi_{xxy} = 0, \end{aligned} \tag{4}$$

then, integrate once with respect to x, namely

$$\phi_{xx} + \phi_{zt} + \phi_{yt} + \phi_{xxxy} + 3\phi_{xx}\phi_{xy} = 0, \tag{5}$$

by setting $\phi = 2\ln f(x, y, z, t)$, Eq. (2) is reduced into the following bilinear equation:

$$\begin{aligned} &B_{\mathrm{gBLMP}}(f) := ff_{xx} - {f_x}^2 + ff_{zt} - f_z f_t \\ &\quad + ff_{yt} - f_y f_t + ff_{xxxy} - f_{xxx}f_y - 3f_x f_{xxy} + 3f_{xx}f_{xy} = 0. \end{aligned} \tag{6}$$

Bilinear Eq. (6) can be turned into the following form:

$$B_{\mathrm{gBLMP}}(f) := (D_x^3 D_y + D_y D_t + D_z D_t + D_x^2) f \cdot f = 0, \tag{7}$$

where D_x, D_y, D_z and D_t are bilinear operators, defined by [8–13,16,17]

$$\prod_{i=1}^{4} D_{\theta_i}^{\xi_i} f \cdot g = \prod_{i=1}^{4} \left(\frac{\partial}{\partial \theta_i} - \frac{\partial}{\partial \theta_i'} \right)^{\xi_i} f(\theta) g(\theta') \Big|_{\theta' = \theta}. \tag{8}$$

where the vectors $\theta = (x, y, z, t)$, $\theta' = (x', y', z', t')$ and $\xi = (\xi_1, \xi_2, \xi_3, \xi_4)$ are arbitrary nonnegative integers. To our knowledge, there are no studies that have been done to solve the (3+1)-dimensional gBLMP Eq. (2) based on the bilinear form Eq. (7).

In this paper, we introduce a multilayer neural network model based on the generalized bilinear form of the (3+1)-dimensional gBLMP Eq. (2) to construct new types of exact network model solutions. The rest of the paper is organized as follows. In Sect. 2, a (3+1)-dimensional p-gBLMP equation and its generalized bilinear form are proposed. Section 3 provides a multilayer neural network model, and gives some explanations for the presented tensor formula. In Sect. 4, some different kinds of exact network model solutions of p-gBLMP equation are constructed through four types of tensor functions. Finally, we conclude our work in Sect. 5.

2 A generalized bilinear equation and its nonlinear counterpart

In the next moment, motivated from Eq. (7), we discuss and solve the following generalized bilinear equation

$$\begin{aligned} &B_{p\text{-gBLMP}}(f) := (D_{p,x}^3 D_{p,y} + D_{p,y} D_{p,t} \\ &\quad + D_{p,z} D_{p,t} + D_{p,x}^2) f \cdot f = 0, \end{aligned} \tag{9}$$

where $D_{p,x}$, $D_{p,y}$, $D_{p,z}$ and $D_{p,t}$ are generalized bilinear operators, defined by [21]

$$\prod_{i=1}^{M} D_{p,\xi_i}^{\theta_i} f \cdot g = \prod_{i=1}^{M} \left(\frac{\partial}{\partial \xi_i} + \alpha_p \frac{\partial}{\partial \zeta_i} \right)^{\theta_i} f(\xi) g(\zeta) \Big|_{\zeta = \xi}, \tag{10}$$

where the vectors $\xi = (\xi_1, \xi_2, \ldots, \xi_M)$ and $\zeta = (\zeta_1, \zeta_2, \ldots, \zeta_M)$ are M-th variables of the two functions, $\theta = (\theta_1, \theta_2, \ldots, \theta_M)$ are arbitrary nonnegative integers, and p is a prime number. And for an integer M, the M-th power of α_p satisfies the rule

$$\alpha_p^M = (-1)^{r(M)}, \ \text{if } M \equiv r(M) \bmod p, \tag{11}$$

with $0 \le r(M) \le p$.

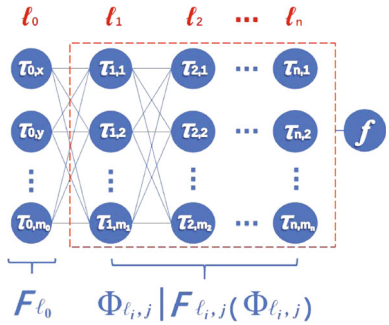

Fig. 1 Multilayer neural network model: ℓ_0 is the input layer; ℓ_i $(i = 1, 2, \ldots, n)$ are the hidden layers; f is the output layer

Remark 2.1 The generalized bilinear differential operators (10) are Hirota bilinear operators (8) when $p = 2k$ $(k \in N^*)$, namely $D_{2k,\xi_i} = D_{\xi_i}$.

If $p = 3$, Eq. (9) reads

$$B_{p\text{-gBLMP}}(f) := 3f_{xx}f_{xy} + ff_{ty} - f_tf_y + ff_{tz} - f_tf_z + ff_{xx} - f_x^2 = 0, \tag{12}$$

where $f = f(x, y, z, t)$ is a new unknown function. Through the link $f = \exp(\int(-u/2)dx)$ as a characteristic transformation in establishing Bell polynomial theories of integrable equations [22], the $B_{p\text{-gBLMP}}$ Eq. (12) is mapped into a (3+1)-dimensional p-gBLMP equation

$$P_{p\text{-gBLMP}}(u) := 3u_x^3u_y - 6u_xu_{xy} - 6u_xu_{xx}u_y + 12u_{xx}u_{xy} - 8u_{xx} - 8u_{ty} - 8u_{tz} = 0. \tag{13}$$

Moreover, the $B_{p\text{-gBLMP}}$ Eq. (12) and the p-gBLMP Eq. (13) satisfy an actual relation, which reads

$$P_{p\text{-gBLMP}}(u) = \left[\frac{8B_{p\text{-gBLMP}}(f)}{f^2}\right]_x, \tag{14}$$

thus, if f is a solution of the $B_{p\text{-gBLMP}}$ Eq. (12), then $u = -2(\ln f)_x$ will solves the p-gBLMP Eq. (13).

3 Multilayer neural network model

In this section, we present a multilayer neural network model to construct exact analytical solutions of Eq. (13), by taking the function f in Eq. (12) as a tensor function in a nonlinear neural network model. The associated neural network model is determined as follows.

Figure 1 shows the structure of the multilayer neural network model, where $\ell_0 = \{\tau_{0,x}, \tau_{0,y}, \ldots, \tau_{0,m_0}\}$, $\ell_1 = \{\tau_{1,1}, \tau_{1,2}, \ldots, \tau_{1,m_1}\}$ and $\ell_i = \{\tau_{i,1}, \tau_{i,2}, \ldots, \tau_{i,m_i}\}$ $(i = 2, 3, \ldots, n)$. And $\ell_n = \{\tau_{n,1}, \tau_{n,2}, \ldots, \tau_{n,m_n}\}$ represents the n-th layer space of the neural network model. The functions $\Phi_{\ell_i,j}$ $(i = 2, 3, \ldots, n)$ $(j = \tau_{i,1}, \tau_{i,2}, \ldots, \tau_{i,m_i})$ in the hidden layers ℓ_i $(i = 2, 3, \ldots, n)$ take expressions in the following form:

$$\Phi_{\ell_i,j} = \sum_{\ell_{i-1}=\tau_{i-1,1}}^{\tau_{i-1,m_{i-1}}} \Theta_{\ell_{i-1},j} \cdot \begin{bmatrix} F_{\tau_{i-1,1}}(\Phi_{\tau_{i-1,1}}) \\ F_{\tau_{i-1,2}}(\Phi_{\tau_{i-1,2}}) \\ \vdots \\ F_{\tau_{i-1,m_{i-1}}}(\Phi_{\tau_{i-1,m_{i-1}}}) \end{bmatrix}^{\mathbf{T}} + \zeta_{\ell_i,j}, \ i = 2, 3, \ldots, n, \tag{15}$$

where $\Theta_{\ell_{i-1},j} = \{\Theta_{\tau_{i-1,1},j}, \Theta_{\tau_{i-1,2},j}, \ldots, \Theta_{\tau_{i-1,m_{i-1}},j}\}$ are the weight coefficients of neurons $\{\tau_{i-1,1}, \tau_{i-1,2}, \ldots, \tau_{i-1,m_{i-1}}\}$ in the hidden layer ℓ_{i-1} to neurons $\{\tau_{i,1}, \tau_{i,2}, \ldots, \tau_{i,m_i}\}$ in the hidden layer ℓ_i. The input layer ℓ_0 and the hidden layer ℓ_1 satisfy $\Phi_{\ell_1,j} = \sum_{\ell_0=\tau_{0,x}}^{\tau_{0,m_0}} \Theta_{\ell_0,j}F_{\ell_0} + \zeta_{\ell_1,j}$ $(j = \tau_{1,1}, \tau_{1,2}, \ldots, \tau_{1,m_1})$, where $F_{\ell_0} \equiv \{x, y, \ldots, m_0\}$. The functions $F_{\ell_i,j}$ $(i = 1, 2, \ldots, n)$ $(j = \tau_{i,1}, \tau_{i,2}, \ldots, \tau_{i,m_i})$ are generalized activation functions, which can be defined arbitrarily. $\zeta_{\ell_i,j}$ $(i = 1, 2, \ldots, n)$ $(j = \tau_{i,1}, \tau_{i,2}, \ldots, \tau_{i,m_i})$ are thresholds, which will be understood as constants in the process of calculation. Moreover, the tensor function f is taken as follows:

$$f = 1 + \sum_{i=1}^{n} \sum_{j=\tau_{i,1}}^{\tau_{i,m_i}} F_j(\Phi_j). \tag{16}$$

In order to further determine the tensor function Eq. (16), we need to select the structure of the neural network $f = \langle m_0, m_1, \ldots, m_n, 1\rangle$, i.e., m_0 neurons in the input layer ℓ_0, m_1 neurons in the hidden layer ℓ_1, m_n neurons in the hidden layer ℓ_n and one neuron in the output layer f.

Remark 3.1 When $n = 1$, Fig. 1 is called a single hidden layer neural network model. Moreover, Eq. (16) can be used to cover many test functions in most analytical solution methods, if we give some specific functions of $F_j(\Phi_j)(j = \tau_{1,1}, \tau_{1,2}, \ldots, \tau_{1,m_1})$.

Remark 3.2 If $n = 1$, $F_j(\Phi_j) = {\zeta_j}^2$ $(j = 1, 2)$, $1 + \sum_{\ell_0=x}^{m_0} \Theta_{\ell_0,j} = C$ $(C \in R, C > 0)$, we have

$$f = {\zeta_1}^2 + {\zeta_2}^2 + C,$$

where $\zeta_j = \Theta_{x,j}x + \Theta_{y,j}y + \Theta_{z,j}z + \Theta_{t,j}t + \Theta_{0,j}$ $(j = 1, 2)$, $\Theta_{x,j}$, $\Theta_{y,j}$, $\Theta_{z,j}$, $\Theta_{t,j}$ and $\Theta_{0,j}$ $(j = 1, 2)$ are real constants, and this is a test function of the lump-type solution [3,4,8–11,16,17].

Remark 3.3 If $n = 1$ and $j = 1, 2, 3$, $F_1(\Phi_1) = \cos(\zeta_1)$, $F_2(\Phi_2) = \cosh(\zeta_2)$, $F_3(\Phi_3) = \exp(\zeta_3)$ and $1 + \sum_{\ell_0=x}^{m_0} \Theta_{\ell_0,j} = C$ ($C \in R, C > 0$), one can be written as

$$f = \cos(\zeta_1) + \cosh(\zeta_2) + \exp(\zeta_3) + C,$$

where $\zeta_j = \Theta_{x,j}x + \Theta_{y,j}y + \Theta_{z,j}z + \Theta_{t,j}t + \Theta_{0,j}$ ($j = 1, 2, 3$). This is a new type of test function to construct the breather lump-stripe (kink) interaction solution [16].

Remark 3.4 If $n = 1$ and $j = 1, 2, 3$, $F_1(\Phi_1) = {\zeta_1}^2$, $F_2(\Phi_2) = \cos(\zeta_2)$, $F_3(\Phi_3) = \exp(\zeta_3)$ and $1 + \sum_{\ell_0=x}^{m_0} \Theta_{\ell_0,j} = C$ ($C \in R, C > 0$), and then Eq. (16) becomes

$$f = {\zeta_1}^2 + \cos(\zeta_2) + \exp(\zeta_3) + C,$$

where $\zeta_j = \Theta_{x,j}x + \Theta_{y,j}y + \Theta_{z,j}z + \Theta_{t,j}t + \Theta_{0,j}$ ($j = 1, 2, 3$). This case can be used to construct the periodic lump-stripe (kink) interaction solution [17].

Acquisition of exact network model solutions. In order to obtain the neural network model solutions of Eq. (13) with the aid of Maple, we take its main steps as follows:

Step 1. Firstly, substituting Eq. (16) into Eq. (12), we determine different polynomial equations of the involved coefficients.

Step 2. Secondly, solving those equations for the coefficients, we can get multi-parameter solutions.

Step 3. Finally, substituting the resulting coefficients into Eq. (16) and further Eq. (3), we obtain exact network model solutions of Eq. (13).

4 Exact network model solutions

In this section, we will construct the exact analytical solutions for Eq. (13) through four types of tensor functions, and give the corresponding dynamic characteristics through some 3D and density plots.

4.1 Bright-dark soliton solutions

If we take $\ell_0 = \{x, y, z, t\}$, $\ell_1 = \{1, 2\}$ and $\ell_2 = \{3, 4, 5\}$, i.e., $f = \langle 4, 2, 3, 1\rangle$, which can be intuitively understood by Fig. 2.

By setting the functions $F_1(\Phi_1) = \cos(\Phi_1), F_2(\Phi_2) = \sin(\Phi_2)$, $F_3(\Phi_3) = \exp(\Phi_3)$, $F_4(\Phi_4) = {\Phi_4}^2$ and $F_5(\Phi_5) = {\Phi_5}^2$, the tensor function f via Eq. (16) can be written as

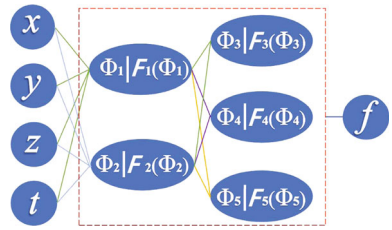

Fig. 2 Case of neural network model $\langle 4, 2, 3, 1\rangle$

$$\begin{cases} f = 1 + \cos(\Phi_1) + \sin(\Phi_2) + \exp(\Phi_3) + {\Phi_4}^2 + {\Phi_5}^2, \\ \Phi_5 = \Theta_{1,5}\cos(\Phi_1) + \Theta_{2,5}\sin(\Phi_2) + \zeta_5, \\ \Phi_4 = \Theta_{1,4}\cos(\Phi_1) + \Theta_{2,4}\sin(\Phi_2) + \zeta_4, \\ \Phi_3 = \Theta_{1,3}\cos(\Phi_1) + \Theta_{2,3}\sin(\Phi_2) + \zeta_3, \\ \Phi_i = x\Theta_{x,i} + y\Theta_{y,i} + z\Theta_{z,i} + t\Theta_{t,i} + \zeta_i, i = 1, 2, \end{cases} \tag{17}$$

where $\Theta_{k,l}(\langle k = x, y, z, t, 1, 2\rangle, \langle l = 1, 2, \ldots, 5\rangle, k \neq l)$ and $\zeta_m (m = 1, 2, \ldots, 5)$ are the undetermined constants. In the general solution procedure, we get the following two sets of solutions of the constant coefficients.

Case 1.

$$\begin{aligned} &\Theta_{1,i} = \Theta_{1,i}(i = 3, 5), \Theta_{2,i} = 0(i = 3, 5), \Theta_{1,4} = \Theta_{1,4}, \\ &\Theta_{2,4} = \Theta_{2,4}, \Theta_{t,1} = \Theta_{t,1}, \Theta_{t,2} = 0, \Theta_{x,1} = \Theta_{x,1}, \\ &\Theta_{x,2} = 0, \Theta_{y,1} = 0, \Theta_{y,2} = -\Theta_{z,2}, \Theta_{z,1} = -\frac{\Theta_{x,1}^2}{\Theta_{t,1}}, \\ &\Theta_{z,2} = \Theta_{z,2}, \zeta_i = \zeta_i(i = 1, 2, \ldots, 5). \end{aligned} \tag{18}$$

Case 2.

$$\begin{aligned} &\Theta_{1,3} = \Theta_{1,3}, \Theta_{1,i} = 0(i = 4, 5), \Theta_{2,3} = 0, \\ &\Theta_{2,i} = \Theta_{2,i}(i = 4, 5), \Theta_{t,1} = \Theta_{t,1}, \Theta_{t,2} = 0, \\ &\Theta_{x,1} = \Theta_{x,1}, \\ &\Theta_{x,2} = 0, \Theta_{y,1} = 0, \Theta_{y,2} = -\Theta_{z,2}, \Theta_{z,1} = -\frac{\Theta_{x,1}^2}{\Theta_{t,1}}, \\ &\Theta_{z,2} = \Theta_{z,2}, \zeta_i = \zeta_i(i = 1, 2, \ldots, 5). \end{aligned} \tag{19}$$

Substituting Eq. (18) into Eq. (17), we generate a solution f, to the $B_{p\text{-gBLMP}}$ Eq. (12); and then, we obtain a solution u to the p-gBLMP Eq. (13) through the transformation Eq. (3), which reads

$$u = \frac{2\Theta_{x,1}\sin(\Phi_1)\left(\Theta_{1,3}e^{\Phi_3} + 2\Theta_{1,5}\Phi_5 + 1\right)}{f}, \tag{20}$$

where f and $\Phi_i (i = 1, 2, \ldots, 5)$ are given as follows:

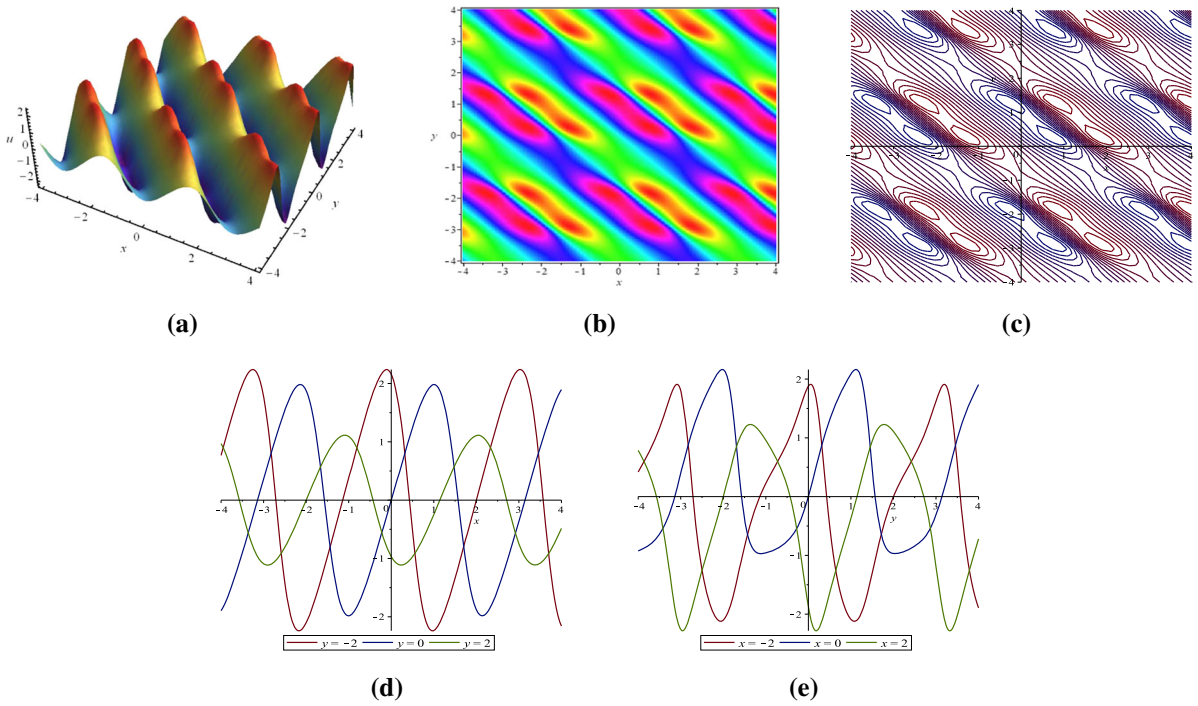

Fig. 3 Profiles of u via (20): **a** 3-D plot, **b** density plot, **c** contour plot, **d** x-curves, **e** y-curves

$$
\begin{aligned}
f &= 1+\cos(\Phi_1)+\sin(\Phi_2)+\exp(\Phi_3)+{\Phi_4}^2+{\Phi_5}^2,\\
\Phi_1 &= \Theta_{x,1}x-\frac{\Theta_{x,1}^2}{\Theta_{t,1}}z+\Theta_{t,1}t+\zeta_1,\\
\Phi_2 &= -\Theta_{z,2}y+\Theta_{z,2}z+\zeta_2,\\
\Phi_3 &= \Theta_{1,3}\cos\left(\Theta_{x,1}x-\frac{\Theta_{x,1}^2}{\Theta_{t,1}}z+\Theta_{t,1}t+\zeta_1\right)+\zeta_3,\\
\Phi_4 &= -\Theta_{2,4}\sin\left(\Theta_{z,2}y-\Theta_{z,2}z-\zeta_2\right)+\zeta_4,\\
\Phi_5 &= \Theta_{1,5}\cos\left(\Theta_{x,1}x-\frac{\Theta_{x,1}^2}{\Theta_{t,1}}z+\Theta_{t,1}t+\zeta_1\right)+\zeta_5.
\end{aligned}
\tag{21}
$$

Figure 3 shows the dynamic characteristics of the exact network model solution (20), by setting different values of the parameters with $t=0$, $z=-y$, $\Theta_{1,3}=-0.1$, $\Theta_{1,5}=0.1$, $\Theta_{2,4}=1$, $\Theta_{t,1}=-2$, $\Theta_{x,1}=-2$, $\Theta_{z,2}=1$ and $\zeta_i=0(i=1,2,\ldots,5)$. It is easy to see that we obtain a type of bright-dark soliton for the p-gBLMP Eq. (13).

4.2 $\langle 4,3,3,1\rangle$ network model solutions

By choosing $\ell_0=\{x,y,z,t\}$, $\ell_1=\{1,2,3\}$ and $\ell_2=\{4,5,6\}$, i.e., $f=\langle 4,3,3,1\rangle$, Fig. 1 can be reduced to Fig. 4.

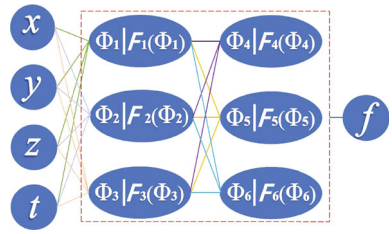

Fig. 4 Case of neural network model $\langle 4,3,3,1\rangle$

According to the above model $\langle 4,3,3,1\rangle$ and tensor formula (16), one can be written as

$$
\begin{cases}
f=1+F_1(\Phi_1)+F_2(\Phi_2)+F_3(\Phi_3)+F_4(\Phi_4)+F_5(\Phi_5)+F_6(\Phi_6),\\
\Phi_6=\Theta_{1,6}F_1(\Phi_1)+\Theta_{2,6}F_2(\Phi_2)+\Theta_{3,6}F_3(\Phi_3)+\zeta_6,\\
\Phi_5=\Theta_{1,5}F_1(\Phi_1)+\Theta_{2,5}F_2(\Phi_2)+\Theta_{3,5}F_3(\Phi_3)+\zeta_5,\\
\Phi_4=\Theta_{1,4}F_1(\Phi_1)+\Theta_{2,4}F_2(\Phi_2)+\Theta_{3,4}F_3(\Phi_3)+\zeta_4,\\
\Phi_i=x\Theta_{x,i}+y\Theta_{y,i}+z\Theta_{z,i}+t\Theta_{t,i}+\zeta_i,\ i=1,2,3,
\end{cases}
\tag{22}
$$

where $\Theta_{k,l}(\langle k=x,y,z,t,1,2,3\rangle,\langle l=1,2,\ldots,6\rangle,k\neq l)$ and $\zeta_m(m=1,2,\ldots,6)$ are the undetermined constants. In a similar way, we can obtain the following cases for solutions of the constant coefficients.

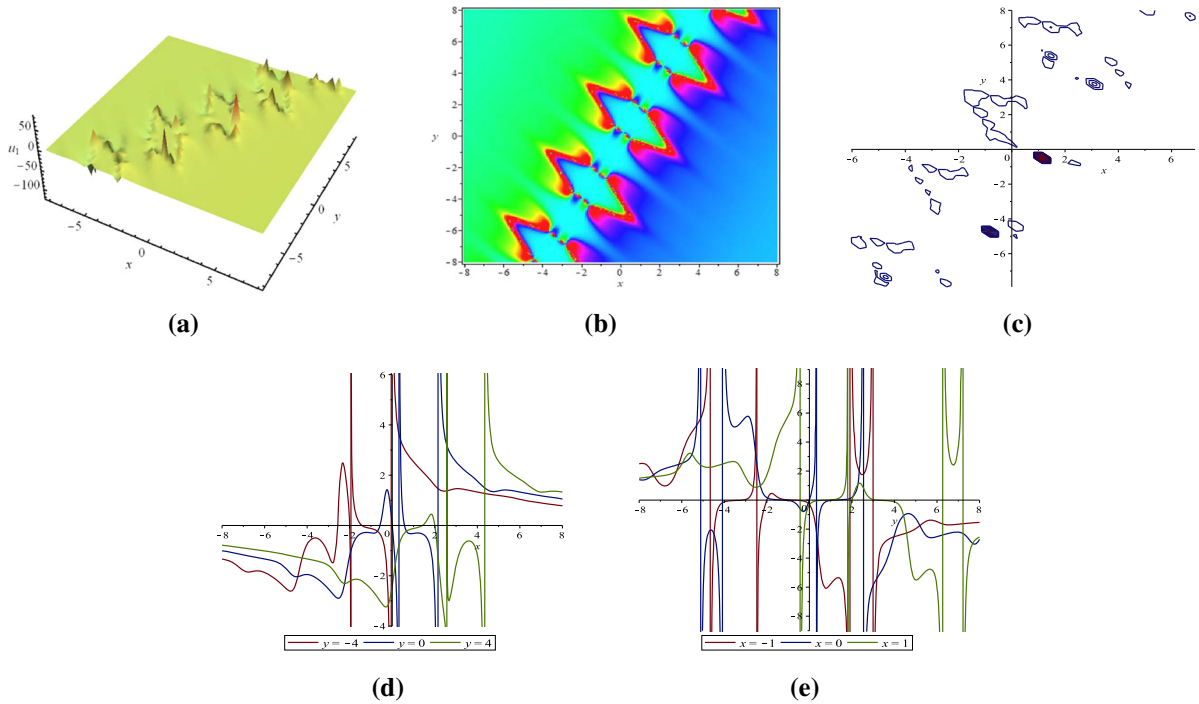

Fig. 5 Profiles of u_1 via (27): **a** 3D plot, **b** density plot, **c** contour plot, **d** x-curves, **e** y-curves

Case 1.

$$\begin{aligned}
&\Theta_{1,i} = \Theta_{1,i}(i = 4, 5),\ \Theta_{2,i} = 0(i = 4, 5),\\
&\Theta_{3,i} = \Theta_{3,i}(i = 4, 5),\ \Theta_{1,6} = 0,\ \Theta_{2,6} = \Theta_{2,6},\ \Theta_{3,6} = 0,\\
&\Theta_{t,1} = \Theta_{t,1},\ \Theta_{t,2} = 0,\ \Theta_{t,3} = -\frac{\Theta_{t,1}^2\Theta_{z,3}}{\Theta_{x,1}^2},\\
&\Theta_{x,1} = \Theta_{x,1},\ \Theta_{x,2} = 0,\ \Theta_{x,3} = -\frac{\Theta_{t,1}\Theta_{z,3}}{\Theta_{x,1}},\ \Theta_{y,1} = 0,\\
&\Theta_{y,2} = -\Theta_{z,2},\ \Theta_{y,3} = 0,\ \Theta_{z,1} = -\frac{\Theta_{x,1}^2}{\Theta_{t,1}},\\
&\Theta_{z,i} = \Theta_{z,i}(i = 2, 3),\ \zeta_i = \zeta_i(i = 1, 2, \ldots, 6).
\end{aligned} \tag{23}$$

Case 2.

$$\begin{aligned}
&\Theta_{1,i} = \Theta_{1,i}(i = 5, 6),\ \Theta_{2,i} = 0(i = 4, 5),\\
&\Theta_{3,i} = 0(i = 5, 6),\ \Theta_{1,4} = 0,\ \Theta_{2,6} = \Theta_{2,6},\ \Theta_{3,4} = \Theta_{3,4},\\
&\Theta_{t,1} = \Theta_{t,1},\ \Theta_{t,2} = -\frac{\Theta_{t,1}^2\Theta_{z,2}}{\Theta_{x,1}^2},\ \Theta_{t,3} = 0,\\
&\Theta_{x,1} = \Theta_{x,1},\ \Theta_{x,2} = -\frac{\Theta_{t,1}\Theta_{z,2}}{\Theta_{x,1}},\ \Theta_{x,3} = 0,\ \Theta_{y,1} = 0,\\
&\Theta_{y,2} = 0,\ \Theta_{y,3} = -\Theta_{z,3},\ \Theta_{z,1} = -\frac{\Theta_{x,1}^2}{\Theta_{t,1}},\\
&\Theta_{z,i} = \Theta_{z,i}(i = 2, 3),\ \zeta_i = \zeta_i(i = 1, 2, \ldots, 6).
\end{aligned} \tag{24}$$

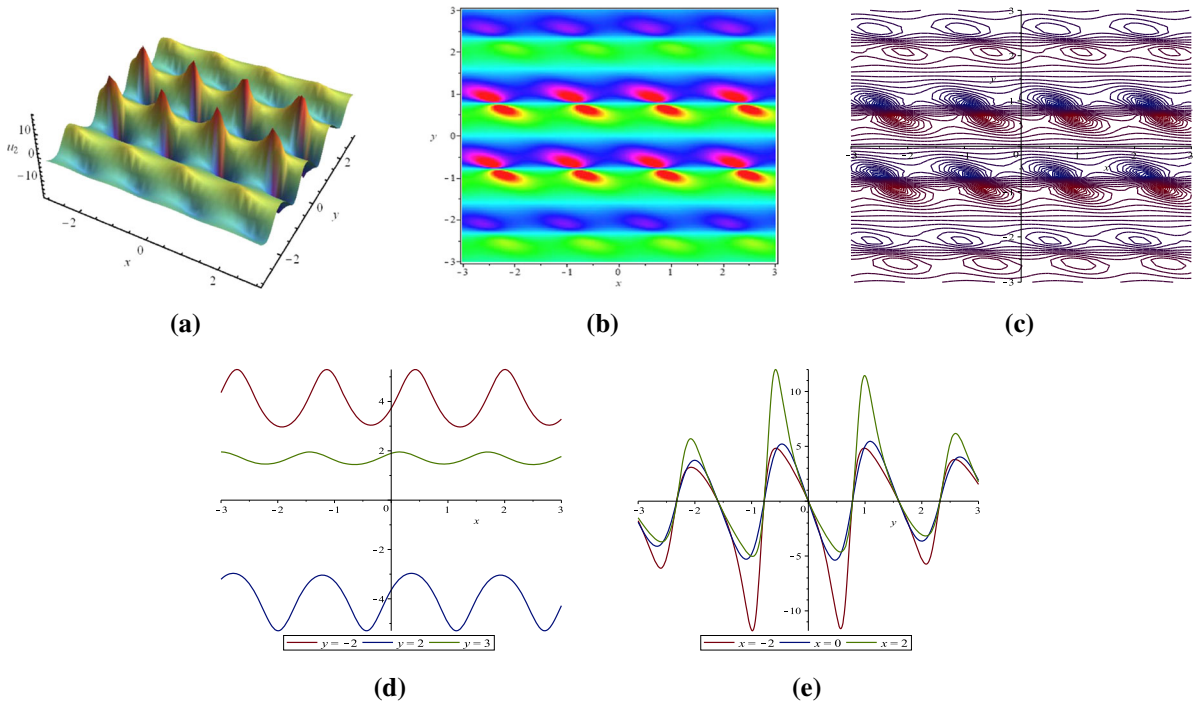

Fig. 6 Profiles of u_2 via (28): **a** 3D plot, **b** density plot, **c** contour plot, **d** x-curves, **e** y-curves

Next, we choose $F_i(\Phi_i)(i = 1, 2, \ldots, 6)$ as some particular functions, then the corresponding tensor functions are shown as below:

$$f_1 = 1 + {\Phi_1}^2 + \sin(\Phi_2) + \cos(\Phi_3) + {\Phi_4}^2 + \cosh(\Phi_5) + \sinh(\Phi_6), \tag{25}$$

$$f_2 = 1 + {\Phi_1}^2 + \sin(\Phi_2) + \cos(\Phi_3) + {\Phi_4}^2 + {\Phi_5}^2 + {\Phi_6}^2, \tag{26}$$

then, substituting Eq. (23) into Eqs. (25) and (26), respectively, we generate two solutions $f_j(j = 1, 2)$, to the $B_{p\text{-gBLMP}}$ Eq. (12). Therefore, we can obtain the following two solutions $u_j(j = 1, 2)$ to p-gBLMP Eq. (13) through the transformation Eq. (3).

$$\begin{aligned} u_1 = \frac{1}{\Theta_{x,1} f_1}\Big(&2\Theta_{3,5}\Theta_{t,1}\Theta_{z,3}\sin(-\Phi_3)\sinh(\Phi_5) \\ &+ 4\Theta_{3,4}\Theta_{t,1}\Theta_{z,3}\Phi_4\sin(-\Phi_3) \\ &- 4\Theta_{1,5}{\Theta_{x,1}}^2\Phi_1\sinh(\Phi_5) - 8\Theta_{1,4}{\Theta_{x,1}}^2\Phi_1\Phi_4 \\ &+ 2\Theta_{t,1}\Theta_{z,3}\sin(-\Phi_3) - 4{\Theta_{x,1}}^2\Phi_1\Big), \end{aligned} \tag{27}$$

$$\begin{aligned} u_2 = \frac{1}{\Theta_{x,1} f_2}\Big(&4\Theta_{3,4}\Theta_{t,1}\Theta_{z,3}\Phi_4\sin(-\Phi_3) \\ &+ 4\Theta_{3,5}\Theta_{t,1}\Theta_{z,3}\Phi_5\sin(-\Phi_3) \\ &- 8\Theta_{1,4}{\Theta_{x,1}}^2\Phi_1\Phi_4 - 8\Theta_{1,5}{\Theta_{x,1}}^2\Phi_1\Phi_5 \\ &+ 2\Theta_{t,1}\Theta_{z,3}\sin(-\Phi_3) - 4{\Theta_{x,1}}^2\Phi_1\Big), \end{aligned} \tag{28}$$

where $\Phi_i(i = 1, 2, \ldots, 6)$ are given as follows:

$$\begin{aligned} \Phi_1 &= \Theta_{x,1}x - \frac{\Theta_{x,1}^2}{\Theta_{t,1}}z + \Theta_{t,1}t + \zeta_1, \\ \Phi_2 &= -\Theta_{z,2}y + \Theta_{z,2}z + \zeta_2, \\ \Phi_3 &= -\frac{\Theta_{t,1}\Theta_{z,3}}{\Theta_{x,1}}x + \Theta_{z,3}z - \frac{\Theta_{t,1}^2\Theta_{z,3}}{\Theta_{x,1}^2}t + \zeta_3, \\ \Phi_4 &= \Theta_{1,4}\Big(\Theta_{x,1}x - \frac{\Theta_{x,1}^2}{\Theta_{t,1}}z + \Theta_{t,1}t + \zeta_1\Big)^2 \\ &\quad + \Theta_{3,4}\cos\Big(\frac{\Theta_{t,1}\Theta_{z,3}}{\Theta_{x,1}}x - \Theta_{z,3}z + \frac{\Theta_{t,1}^2\Theta_{z,3}}{\Theta_{x,1}^2}t - \zeta_3\Big) + \zeta_4, \\ \Phi_5 &= \Theta_{1,5}\Big(\Theta_{x,1}x - \frac{\Theta_{x,1}^2}{\Theta_{t,1}}z + \Theta_{t,1}t + \zeta_1\Big)^2 \\ &\quad + \Theta_{3,5}\cos\Big(\frac{\Theta_{t,1}\Theta_{z,3}}{\Theta_{x,1}}x - \Theta_{z,3}z + \frac{\Theta_{t,1}^2\Theta_{z,3}}{\Theta_{x,1}^2}t - \zeta_3\Big) + \zeta_5, \\ \Phi_6 &= -\Theta_{2,6}\sin(\Theta_{z,2}y - \Theta_{z,2}z - \zeta_2) + \zeta_6. \end{aligned} \tag{29}$$

Figure 5 shows the special interaction structures expressed by (27), which can be summed up as a kind of rogue wave phenomenon, with the parameters being

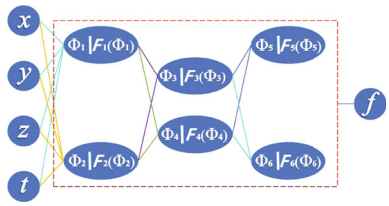

Fig. 7 Case of neural network model ⟨4, 2, 2, 2, 1⟩

fixed by $t = -y$, $z = -x$, $\Theta_{1,4} = -1$, $\Theta_{1,5} = 0.1$, $\Theta_{2,6} = -4, \Theta_{3,i} = 1 (i = 4, 5), \Theta_{t,1} = 1, \Theta_{x,1} = -2$, $\Theta_{z,2} = 1$, $\Theta_{z,3} = 1$ and $\zeta_i = 0 (i = 1, 2, \ldots, 6)$. Figure 6 shows the dynamic characteristics of the exact network model solution (28), which is a new type of multiple periodic lump wave, by setting values of the parameters with $t = y, z = -x, \Theta_{1,4} = -0.01, \Theta_{1,5} = 0.01$, $\Theta_{2,6} = 6$, $\Theta_{3,i} = 6 (i = 4, 5)$, $\Theta_{t,1} = 2$, $\Theta_{x,1} = -2$, $\Theta_{z,2} = 2$, $\Theta_{z,3} = -2$ and $\zeta_i = 0 (i = 1, 2, \ldots, 6)$.

4.3 ⟨4, 2, 2, 2, 1⟩ network model solutions

If we select $\ell_0 = \{x, y, z, t\}$, $\ell_1 = \{1, 2\}$, $\ell_2 = \{3, 4\}$ and $\ell_3 = \{5, 6\}$, i.e., $f = \langle 4, 2, 2, 2, 1 \rangle$, which can be intuitively understood by Fig. 7.
By setting the functions $F_1(\Phi_1) = {\Phi_1}^2$, $F_2(\Phi_2) = {\Phi_2}^2$, $F_3(\Phi_3) = \cos(\Phi_3)$, $F_4(\Phi_4) = \cosh(\Phi_4)$, $F_5(\Phi_5) = \Phi_5$ and $F_6(\Phi_6) = \Phi_6$, then the tensor function f via Eq. (16) has the following form:

$$\begin{cases} f = 1 + {\Phi_1}^2 + {\Phi_2}^2 + \cos(\Phi_3) + \cosh(\Phi_4) + \Phi_5 + \Phi_6, \\ \Phi_i = \Theta_{3,i} \cos(\Phi_3) + \Theta_{4,i} \cosh(\Phi_4) + \zeta_i, i = 5, 6, \\ \Phi_j = \Theta_{1,j} {\Phi_1}^2 + \Theta_{2,j} {\Phi_2}^2 + \zeta_j, j = 3, 4, \\ \Phi_2 = x\Theta_{x,2} + y\Theta_{y,2} + z\Theta_{z,2} + t\Theta_{t,2} + \zeta_2, \\ \Phi_1 = x\Theta_{x,1} + y\Theta_{y,1} + z\Theta_{z,1} + t\Theta_{t,1} + \zeta_1, \end{cases} \tag{30}$$

where $\Theta_{k,l} (\langle k = x, y, z, t, 1, 2, 3, 4 \rangle, \langle l = 1, 2, \ldots, 6 \rangle, k \neq l)$ and $\zeta_m (m = 1, 2, \ldots, 6)$ are the undetermined constants. Substituting Eq. (30) into $B_{p\text{-gBLMP}}$ Eq. (12) in the same way, we also can obtain two solutions of the constant coefficients as follows:

Case 1.

$$\begin{aligned} &\Theta_{1,3} = 0, \Theta_{1,4} = \Theta_{1,4}, \Theta_{2,4} = \Theta_{3,6} = \Theta_{4,5} = 0, \\ &\Theta_{2,3} = \Theta_{2,3}, \Theta_{3,5} = \Theta_{3,5}, \\ &\Theta_{4,6} = \Theta_{4,6}, \Theta_{t,1} = \Theta_{t,1}, \Theta_{t,2} = 0, \Theta_{x,1} = \Theta_{x,1}, \\ &\Theta_{x,2} = 0, \Theta_{y,1} = 0, \\ &\Theta_{y,2} = -\Theta_{z,2}, \Theta_{z,1} = -\frac{{\Theta_{x,1}}^2}{\Theta_{t,1}}, \Theta_{z,2} = \Theta_{z,2}, \\ &\zeta_i = \zeta_i (i = 1, 2, \ldots, 6). \end{aligned} \tag{31}$$

Case 2.

$$\begin{aligned} &\Theta_{1,3} = \Theta_{1,3}, \Theta_{1,4} = 0, \Theta_{2,4} = \Theta_{2,4}, \\ &\Theta_{3,5} = \Theta_{4,6} = \Theta_{2,3} = 0, \Theta_{3,6} = \Theta_{3,6}, \\ &\Theta_{4,5} = \Theta_{4,5}, \Theta_{t,1} = 0, \Theta_{t,2} = \Theta_{t,2}, \\ &\Theta_{x,1} = 0, \Theta_{x,2} = \Theta_{x,2}, \Theta_{y,1} = -\Theta_{z,1}, \\ &\Theta_{y,2} = 0, \Theta_{z,1} = \Theta_{z,1}, \Theta_{z,2} = -\frac{{\Theta_{x,2}}^2}{\Theta_{t,2}}, \\ &\zeta_i = \zeta_i (i = 1, 2, \ldots, 6). \end{aligned} \tag{32}$$

Equations (28) and (29) generate two types of tensor function solutions $f_j (j = 1, 2)$, defined by (30), to $B_{p\text{-gBLMP}}$ Eq. (12); and further the resulting tensor functions present two types of network model solutions $u_j (j = 1, 2)$ to p-gBLMP Eq. (13), under the transformation Eq. (3). For the first set of parametric solutions Eq. (31), we have

$$u = -\frac{4\Theta_{x,1}\Phi_1 \left(\Theta_{1,4}\Theta_{4,6} \sinh(\Phi_4) + \Theta_{1,4} \sinh(\Phi_4) + 1\right)}{f}, \tag{33}$$

where $\Phi_i (i = 1, 2, \ldots, 6)$ are given as follows:

$$\begin{aligned} \Phi_1 &= \Theta_{x,1}x - \frac{{\Theta_{x,1}}^2}{\Theta_{t,1}}z + \Theta_{t,1}t + \zeta_1, \\ \Phi_2 &= -\Theta_{z,2}y + \Theta_{z,2}z + \zeta_2, \\ \Phi_3 &= \Theta_{2,3}\left(-\Theta_{z,2}y + \Theta_{z,2}z + \zeta_2\right)^2 + \zeta_3, \\ \Phi_4 &= \Theta_{1,4}\left(\Theta_{x,1}x - \frac{{\Theta_{x,1}}^2}{\Theta_{t,1}}z + \Theta_{t,1}t + \zeta_1\right)^2 + \zeta_4, \\ \Phi_5 &= \Theta_{3,5} \cos\left(\Theta_{2,3}\left(-\Theta_{z,2}y + \Theta_{z,2}z + \zeta_2\right)^2 + \zeta_3\right) + \zeta_5, \\ \Phi_6 &= \Theta_{4,6} \cosh\left(\Theta_{1,4}\left(\Theta_{x,1}x - \frac{{\Theta_{x,1}}^2}{\Theta_{t,1}}z + \Theta_{t,1}t + \zeta_1\right)^2 \right. \\ &\quad \left. + \zeta_4\right) + \zeta_6. \end{aligned} \tag{34}$$

The 3D dynamic, density, contour, x-curves and y-curves graphs of the network model solution (33) are successfully depicted in Fig. 8, by setting the values of $\Theta_{k,l} (\langle k = x, y, z, t, 1, 2, 3, 4 \rangle, \langle l = 1, 2, \ldots, 6 \rangle, k \neq l)$ and $\zeta_k (k = 1, 2, \ldots, 6)$ in Eq. (33) as

$$\begin{aligned} &t = y, z = -x, \Theta_{1,4} = -0.01, \Theta_{2,3} = 0.01, \\ &\Theta_{3,5} = 1, \Theta_{4,6} = 1, \\ &\Theta_{x,1} = 1, \Theta_{z,2} = 1, \Theta_{t,1} = -2, \zeta_i = 0 (i = 1, 2, \ldots, 6). \end{aligned} \tag{35}$$

5 Conclusions

In this study, we obtained a (3+1)-dimensional p-gBLMP equation through the mapping transformation

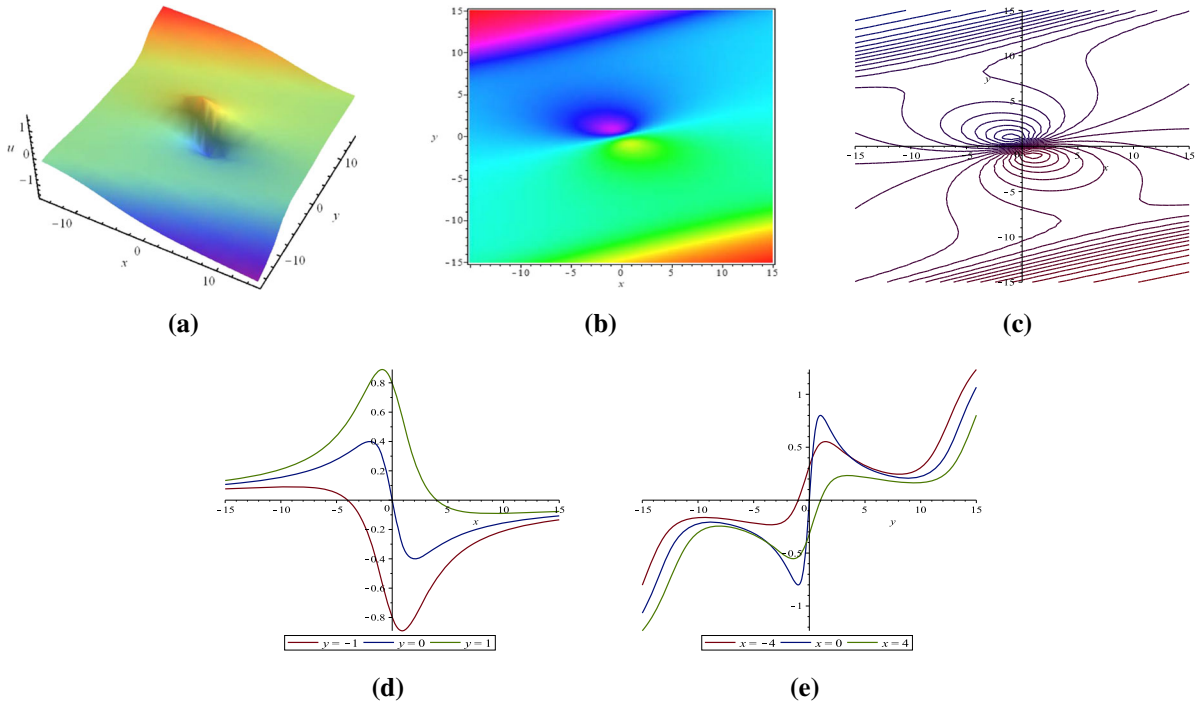

Fig. 8 Profiles of u via (33): **a** 3D plot, **b** density plot, **c** contour plot, **d** x-curves, **e** y-curves

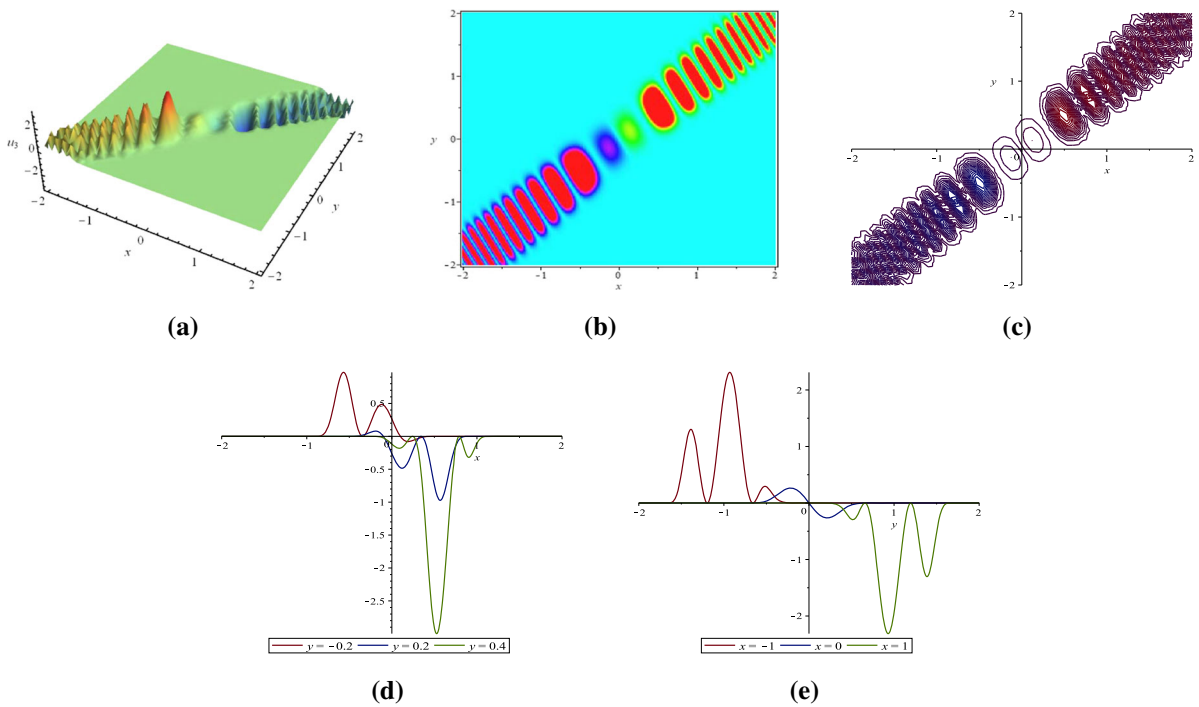

Fig. 9 Profiles of u_3 via (37) with $t = -y$, $z = x$, $\Theta_{1,4} = -1$, $\Theta_{1,5} = 1$, $\Theta_{2,6} = 1$, $\Theta_{3,i} = 1 (i = 4, 5)$, $\Theta_{t,1} = 1$, $\Theta_{x,1} = -1$, $\Theta_{z,2} = 4$, $\Theta_{z,3} = 1$ and $\zeta_i = 0 (i = 1, 2, \ldots, 6)$: **a** 3D plot, **b** density plot, **c** contour plot, **d** x-curves, **e** y-curves

of a $B_{p\text{-gBLMP}}$ equation, based on the generalized bilinear differential operators. Then, the multilayer neural network model was given completely and applied to solve the p-gBLMP equation successfully.

We constructed four types of network model solutions for the p-gBLMP equation, by utilizing three structures of the multilayer neural network model. For the first case of $\langle 4, 2, 3, 1\rangle$, we have given a kind of tensor formula and obtained a type of bright-dark soliton solution (see Fig. 3) of the p-gBLMP equation. In the $\langle 4, 3, 3, 1\rangle$ network model, two types of tensor formulas were proposed, and we presented a kind of rogue wave solution (see Fig. 5) and a new type of multiple periodic lump wave solution (see Fig. 6), respectively. For the third network model $\langle 4, 2, 2, 2, 1\rangle$, we obtained a type of interaction solution (see Fig. 8) through one tensor formula. Hope these novel findings can promote the understanding of the (3+1)-dimensional gBLMP and p-gBLMP equations.

Therefore, it is feasible and effective to construct new exact analytical solutions of nonlinear PDEs by using the multilayer neural network model. It should be particularly interesting to note that by setting the hidden neurons in one same network model to some different functions, many different types of network model solutions can be obtained. Such as the case of the neural network model $\langle 4, 3, 3, 1\rangle$ in Fig. 4, a third network model solution (see Fig. 9) for the p-gBLMP Eq. (13) can also be given if we choose the following tensor formula

$$f_3 = 1 + {\Phi_1}^2 + {\Phi_2}^2 + {\Phi_3}^2 + \exp(-\Phi_4) + \cos(\Phi_5) + \exp(\Phi_6), \tag{36}$$

and then, one can be written as

$$\begin{aligned} u_3 = \frac{4}{\Theta_{x,1} f_3}\Big(&\Theta_{1,4}{\Theta_{x,1}}^2\Phi_1 e^{-\Theta_{1,4}{\Phi_1}^2-\Theta_{3,4}{\Phi_3}^2-\zeta_4} \\ &-\Theta_{3,4}\Theta_{t,1}\Theta_{z,3}\Phi_3 e^{-\Theta_{1,4}{\Phi_1}^2-\Theta_{3,4}{\Phi_3}^2-\zeta_4} \\ &+\Theta_{1,5}{\Theta_{x,1}}^2\Phi_1\sin(\Phi_5) - \Theta_{3,5}\Theta_{t,1}\Theta_{z,3}\Phi_3\sin(\Phi_5) \\ &+\Theta_{t,1}\Theta_{z,3}\Phi_3 - {\Theta_{x,1}}^2\Phi_1\Big), \end{aligned} \tag{37}$$

where $\Phi_i (i = 1, 2, \ldots, 6)$ are given as follows:

$$\begin{aligned} \Phi_1 &= \Theta_{x,1}x - \frac{\Theta_{x,1}^2}{\Theta_{t,1}}z + \Theta_{t,1}t + \zeta_1, \\ \Phi_2 &= -\Theta_{z,2}y + \Theta_{z,2}z + \zeta_2, \\ \Phi_3 &= -\frac{\Theta_{t,1}\Theta_{z,3}}{\Theta_{x,1}}x + \Theta_{z,3}z - \frac{\Theta_{t,1}^2\Theta_{z,3}}{\Theta_{x,1}^2}t + \zeta_3, \\ \Phi_4 &= \Theta_{1,4}\Big(\Theta_{x,1}x - \frac{\Theta_{x,1}^2}{\Theta_{t,1}}z + \Theta_{t,1}t + \zeta_1\Big)^2 \\ &\quad + \Theta_{3,4}\Big(-\frac{\Theta_{t,1}\Theta_{z,3}}{\Theta_{x,1}}x + \Theta_{z,3}z - \frac{\Theta_{t,1}^2\Theta_{z,3}}{\Theta_{x,1}^2}t + \zeta_3\Big)^2 + \zeta_4, \\ \Phi_5 &= \Theta_{1,5}\Big(\Theta_{x,1}x - \frac{\Theta_{x,1}^2}{\Theta_{t,1}}z + \Theta_{t,1}t + \zeta_1\Big)^2 \\ &\quad + \Theta_{3,5}\Big(-\frac{\Theta_{t,1}\Theta_{z,3}}{\Theta_{x,1}}x + \Theta_{z,3}z - \frac{\Theta_{t,1}^2\Theta_{z,3}}{\Theta_{x,1}^2}t + \zeta_3\Big)^2 + \zeta_5, \\ \Phi_6 &= \Theta_{2,6}(-\Theta_{z,2}y + \Theta_{z,2}z + \zeta_2)^2 + \zeta_6. \end{aligned} \tag{38}$$

Moreover, by taking other different structures of the neural network $f = \langle m_0, m_1, \ldots, m_n, 1\rangle$, we can obtain much more types of tensor functions of the neural network model, for which the corresponding network model solutions of the (3+1)-dimensional p-gBLMP equation can be similarly generated.

Acknowledgements The work was supported in part by NSFC (11371326, 11301331, 11371086, 11571079, 51771083 and 11661060), NSF under the grant DMS-1664561, Natural Science Fund for Colleges and Universities of Jiangsu Province under the Grant 17KJB110020, Emphasis Foundation of Special Science Research on Subject Frontiers of CUMT under Grant No. 2017XKZD11, and Program for Young Talents of Science and Technology in Universities of Inner Mongolia Autonomous Region (NJYT-20-A06).

Data availability Data sharing is not applicable to this article as no datasets were generated or analyzed during the current study.

Declarations

Conflict of interest The authors declare that they have no conflict of interest.

References

1. Chen, Y., Khater, M.M.A., Inc, M., Attia, R.A.M., Lu, D.C.: Abundant analytical solutions of the fractional nonlinear (2+1)-dimensional BLMP equation arising in incompressible fluid. Int. J. Mod. Phys. B. **34**, 2050084 (2020)
2. Liu, J.G., Zhu, W.H., He, Y., Seadawy, A.R.: Complexiton solutions and periodic-soliton solutions for the (2+1)-dimensional BLMP equation. AIMS Math. **5**, 421–439 (2020)
3. He, C.H., Tang, Y.N., Ma, W.X., Ma, J.L.: Interaction phenomena between a lump and other multi-solitons for the

(2+1)-dimensional BLMP and Ito equations. Nonlinear Dyn. **95**, 29–42 (2019)
4. Kaplan, M.: Two different systematic techniques to find analytical solutions of the (2+1)-dimensional Boiti–Leon–Manna–Pempinelli equation. Chin. J. Phys. **56**, 2523–2530 (2018)
5. Kaplan, M., Akbulut, A., Bekir, A.: The Auto-Bäcklund transformations for the (2+1)-dimensional Boiti–Leon–Manna–Pempinelli equation. AIP Conf. Proc. **1798**, 020071 (2017)
6. Kaplan, M., Ozer, M.N.: Multiple-soliton solutions and analytical solutions to a nonlinear evolution equation. Opt. Quant. Electron. **50**, 2 (2018)
7. Kaplan, M., Ozer, M.N.: Auto-Bäcklund transformations and solitary wave solutions for the nonlinear evolution equation. Opt. Quant. Electron. **50**, 33 (2018)
8. Muhammad, H., Muhammad, U., Tamour, Z., Rizwan, U.H., Ahmad, S.: An efficient analysis for N-soliton, Lump and lump-kink solutions of time-fractional (2+1)-Kadomtsev–Petviashvili equation. Physica A **528**, 121320 (2019)
9. Ma, W.X., Zhou, Y.: Lump solutions to nonlinear partial differential equations via Hirota bilinear forms. J. Differ. Equ. **264**, 2633–2659 (2018)
10. Ma, W.X., Manukure, S., Wang, H., Batwa, S.: Lump solutions to a (2+1)-dimensional fourth-order nonlinear PDE possessing a Hirota bilinear form. Mod. Phys. Lett. B. **35**, 2150160 (2021)
11. Ma, W.X., Bai, Y.S., Adjiri, A.: Nonlinearity-managed lump waves in a spatial symmetric HSI model. Eur. Phys. J. Plus **136**, 240 (2021)
12. Wazwaz, A.M.: Multiple soliton solutions for the Bogoyavlenskii's generalized breaking soliton equations and its extension form. Appl. Math. Comput. **217**, 4282–4288 (2010)
13. Liu, J.G., Zhou, L., He, Y.: Multiple soliton solutions for the new (2+1)-dimensional Korteweg–de Vries equation by multiple exp-function method. Appl. Math. Lett. **80**, 71–78 (2018)
14. Zhang, Y., Liu, Y.P., Tang, X.Y.: M-lump and interactive solutions to a (3+1)-dimensional nonlinear system. Nonlinear Dyn. **93**, 2533–2541 (2018)
15. Zhang, Y., Liu, Y.P., Tang, X.Y.: M-lump solutions to a (3+1)-dimensional nonlinear evolution equation. Comput. Math. Appl. **76**, 592–601 (2018)
16. Gai, L.T., Ma, W.X., Li, M.C.: Lump-type solution and breather lump-kink interaction phenomena to a (3+1)-dimensional GBK equation based on trilinear form. Nonlinear Dyn. **100**, 2715–2727 (2020)
17. Gai, L.T., Ma, W.X., Li, M.C.: Lump-type solutions, rogue wave type solutions and periodic lump-stripe interaction phenomena to a (3+1)-dimensional generalized breaking soliton equation. Phys. Lett. A. **384**, 126178 (2020)
18. Deng, G.F., Gao, Y.T., Su, J.J., Ding, C.C., Jia, T.T.: Solitons and periodic waves for the (2+1)-dimensional generalized Caudrey–Dodd–Gibbon–Kotera–Sawada equation in fluid mechanics. Nonlinear Dyn. **99**, 1039–1052 (2020)
19. Kuo, C.K., Ghanbari, B.: Resonant multi-soliton solutions to new (3+1)-dimensional Jimbo–Miwa equations by applying the linear superposition principle. Nonlinear Dyn. **96**, 459–464 (2019)
20. Wang, M., Tian, B., Sun, Y., Yin, H.M., Zhang, Z.: Mixed lump-stripe, bright rogue wave-stripe, dark rogue wavestripe and dark rogue wave solutions of a generalized Kadomtsev–Petviashvili equation in fluid mechanics. Chin. J. Phys. **60**, 440–449 (2019)
21. Ma, W.X.: Generalized bilinear differential equations. Stud. Nonlinear Sci. **2**, 140–144 (2011)
22. Ma, W.X.: Bilinear equations, Bell polynomials and linear superposition principle. J. Phys.: Conf. Ser. **411**, 012021 (2013)